JCI The Journal of Clinical Investigation

Pex/PEX tissue distribution and evidence for a deletion in the 3' region of the Pex gene in X-linked hypophosphatemic mice.

L Beck, Y Soumounou, J Martel, G Krishnamurthy, C Gauthier, C G Goodyer, H S Tenenhouse

J Clin Invest. 1997;99(6):1200-1209. https://doi.org/10.1172/JCI119276.

Research Article

PEX, a phosphate-regulating gene with homology to endopeptidases on the X chromosome, was recently identified as the candidate gene for X-linked hypophosphatemia. In the present study, we cloned mouse and human Pex/PEX cDNAs encoding part of the 5' untranslated region, the protein coding region, and the entire 3' untranslated region, determined the tissue distribution of Pex/PEX mRNA, and characterized the Pex mutation in the murine Hyp homologue of the human disease. Using the reverse transcriptase/polymerase chain reaction (RT/PCR) and ribonuclease protection assays, we found that Pex/PEX mRNA is expressed predominantly in human fetal and adult mouse calvaria and long bone. With RNA from Hyp mouse bone, an RT/PCR product was generated with 5' but not 3' Pex primer pairs and a protected Pex mRNA fragment was detected with 5' but not 3' Pex riboprobes by ribonuclease protection assay. Analysis of the RT/PCR product derived from Hyp bone RNA revealed an aberrant Pex transcript with retention of intron sequence downstream from nucleotide 1302 of the Pex cDNA. Pex mRNA was not detected on Northern blots of poly (A)+ RNA from Hyp bone, while a low-abundance Pex transcript of approximately 7 kb was apparent in normal bone. Southern analysis of genomic DNA from Hyp mice revealed the absence of hybridizing bands with cDNA probes from the 3' region of the Pex cDNA. […]

Pex/PEX Tissue Distribution and Evidence for a Deletion in the 3′ Region of the *Pex* Gene in X-Linked Hypophosphatemic Mice

Laurent Beck,*‡ Youssouf Soumounou,* Josée Martel,* Ganga Krishnamurthy,* Claude Gauthier,* Cynthia G. Goodyer,* and Harriet S. Tenenhouse*‡

**Department of Pediatrics, McGill University-Montreal Children's Hospital Research Institute, and ‡Department of Human Genetics, McGill University, Montreal, Quebec, 3H3 1P3, Canada*

Abstract

PEX, a phosphate-regulating gene with homology to endopeptidases on the X chromosome, was recently identified as the candidate gene for X-linked hypophosphatemia. In the present study, we cloned mouse and human _Pex/PEX_ cDNAs encoding part of the 5′ untranslated region, the protein coding region, and the entire 3′ untranslated region, determined the tissue distribution of _Pex/PEX_ mRNA, and characterized the _Pex_ mutation in the murine _Hyp_ homologue of the human disease. Using the reverse transcriptase/polymerase chain reaction (RT/PCR) and ribonuclease protection assays, we found that _Pex/PEX_ mRNA is expressed predominantly in human fetal and adult mouse calvaria and long bone. With RNA from _Hyp_ mouse bone, an RT/PCR product was generated with 5′ but not 3′ _Pex_ primer pairs and a protected _Pex_ mRNA fragment was detected with 5′ but not 3′ _Pex_ riboprobes by ribonuclease protection assay. Analysis of the RT/PCR product derived from _Hyp_ bone RNA revealed an aberrant _Pex_ transcript with retention of intron sequence downstream from nucleotide 1302 of the _Pex_ cDNA. _Pex_ mRNA was not detected on Northern blots of poly $(A)^+$ RNA from _Hyp_ bone, while a low-abundance _Pex_ transcript of $\approx$ 7 kb was apparent in normal bone. Southern analysis of genomic DNA from _Hyp_ mice revealed the absence of hybridizing bands with cDNA probes from the 3′ region of the _Pex_ cDNA. We conclude that _Pex/PEX_ is a low-abundance transcript that is expressed predominantly in bone of mice and humans and that a large deletion in the 3′ region of the _Pex_ gene is present in the murine _Hyp_ homologue of X-linked hypophosphatemia. (_J. Clin. Invest._ 1997. 99:1200–1209.) Key words: phosphate • transport • kidney • bone • endopeptidase

Introduction

X-linked hypophosphatemia (XLH)[1] (MIM #307800) is the most frequently occurring form of inherited rickets in humans with an incidence of 1 in 20,000 individuals (1, 2). It is a dominant disorder of phosphate homeostasis characterized by rachitic and osteomalacic bone disease, short stature, hypophosphatemia, and renal defects in phosphate reabsorption and vitamin D metabolism (2). Much of our knowledge of the human disease is derived from studies of the murine *Hyp* mutation (2–5), which maps to a region of the mouse X chromosome that is syntenic to the XLH (*HYP*) locus on the human X chromosome (6). We demonstrated that *Hyp* mice have a specific defect in phosphate transport across the renal brush border membrane that is associated with a decrease in high affinity Na^+-phosphate cotransport V_{max} (7) and can be ascribed to a decrease in renal abundance of type II Na^+-phosphate cotransporter (*Npt2*) mRNA and immunoreactive protein (8). We also showed that the regulation of the vitamin D catabolic enzyme, 1,25-dihydroxyvitamin D-24-hydroxylase, is perturbed in *Hyp* mouse kidney (9–12). However, the *NPT2* and 24-hydroxylase genes have been ruled out as candidate genes for XLH and *Hyp* since both genes map to autosomes (13, 14).

Recently, a candidate gene for XLH was identified by an international consortium using a positional cloning approach (15). The gene was designated *PEX* to signify a Phosphate-regulating gene with homology to Endopeptidases on the X chromosome (15). DNA samples from 150 unrelated individuals with XLH were analyzed; deletions ranging from 1 to 55 kb were identified in four XLH patients and one frameshift and two splice site mutations found in three other individuals (15). More than 20 additional *PEX* mutations have since been reported (16–18), demonstrating molecular heterogeneity for XLH.

The *PEX* gene contains significant homology to a family of metalloprotease genes which include neutral endopeptidase 24.11 (NEP) and endothelin converting enzyme-1 (ECE-1) (15). These are type II integral membrane glycoproteins, characterized by a short cytoplasmic domain, a transmembrane domain, and a large extracellular domain which retains full catalytic activity. In addition to these similarities, the putative extracellular domain of *PEX* has a zinc binding motif that is essential for catalytic activity and conserved cysteine residues that are critical for protein conformation in NEP (15).

The mechanism whereby mutations in *PEX* elicit the XLH phenotype is not clear. It has been demonstrated that NEP is involved in the proteolytic degradation and inactivation of various small peptide mediators (19) whereas ECE-1 plays an important role in the activation of endothelin from an inactive precursor peptide, big endothelin-1 (20). Based on these findings, one can speculate that *PEX* is involved in the processing/degradation of a hormone that is involved in the regulation of renal phosphate handling and the maintenance of phosphate homeostasis.

To understand the physiological role of *PEX*, a knowledge of its tissue distribution is essential. Although the consortium was unable to detect *PEX* mRNA expression on Northern

Address correspondence to Harriet S. Tenenhouse, Montreal Children's Hospital, 2300 Tupper Street, Montreal, Quebec H3H 1P3, Canada. Phone: 514-934-4417; FAX: 514-934-4329; E-mail: mdht@musica.mcgill.ca

Received for publication 22 October 1996 and accepted in revised form 2 January 1997.

1. *Abbreviations used in this paper:* ECE-1, endothelin-converting enzyme 1; NEP, neutral endopeptidase 24.11; RACE, rapid amplification of cDNA ends; UTR, untranslated region; XLH, X-linked hypophosphatemia.

J. Clin. Invest.

0021-9738/97/03/1200/10 $2.00
Volume 99, Number 6, March 1997, 1200–1209

blots from multiple human and mouse tissues (15), a recent study provided evidence for a low-abundance 6.6-kb *Pex* transcript in mouse bone and cultured mouse osteoblasts (21). Of interest was the finding that a *Pex* transcript was not detected in *Hyp* bone (21). The present study was undertaken to clone mouse and human *Pex*/*PEX* (*Pex/PEX* signifies the mouse [*Pex*] and human [*PEX*] genes, cDNAs, transcripts, or proteins) cDNAs, to determine the distribution of *Pex*/*PEX* transcripts in human fetal and murine tissues and to define the nature of the *Pex* mutation in *Hyp* mice. These studies provide a basis for understanding *Pex*/*PEX* function and the mechanism whereby *Pex*/*PEX* mutations perturb phosphate homeostasis, bone mineralization, and growth.

Methods

Human fetal tissues. Tissues from human fetuses (11–22 wk fetal age) were obtained at the time of therapeutic abortion by dilatation and curettage. The samples were flash frozen in a dry ice/acetone bath and stored at −70°C. Fetal age was determined by foot length (22). Protocols for obtaining the fetal tissues were approved by local Institutional Review Boards and informed consent was obtained in all cases.

Mice. Mutant *Hyp* hemizygote and normal male mice, obtained by breeding C57Bl/6J *Hyp*/+ females with C57Bl/6J +/Y males, were used in the present study. The original breeding pairs were obtained from The Jackson Laboratory (Bar Harbor, ME). *Hyp* mice were distinguished from normal littermates by their lower body weight, shorter tail, and hypophosphatemia (3). The mice were maintained on Teklad Rodent Diet (diet no. 8604; Harlan Teklad, Madison, WI) containing 1.2% calcium and 1% Pi. Mouse embryos were harvested at day 18. All experiments were conducted in accordance with the guidelines of the Canadian Council on Animal Care.

Isolation of total and poly(A)$^+$ RNA. Total RNA was extracted from various human fetal and mouse tissues using TRIzol reagent (Gibco-BRL, Burlington, Ontario). Poly(A)$^+$ RNA selection was achieved with oligo(dT_{30}) covalently linked to polystyrene latex beads (Oligotex mRNA kit; Qiagen, Chatsworth, CA), according to the manufacturer's protocol.

Reverse transcriptase (RT)-PCR. Total RNA (5–10 μg) from human fetal and mouse tissues was reverse transcribed using random hexamers and SuperScript reverse transcriptase (Gibco-BRL), as recommended by the manufacturer. PCR was initially performed using primers derived from the human *PEX* sequence (15). Mouse and human *Pex*/*PEX* cDNA sequences, corresponding to nucleotides 142–1914 (numbering refers to the mouse and human *Pex*/*PEX* cDNA sequences [Fig. 1 *A*] with A of the ATG initiation codon designated as one) were derived by sequencing PCR products obtained with the following primer pairs: (*a*) 5′-CAAGCTAAACAGGAGTACTGCC-3′ (F142) and 5′-CCTCTTCCCCTTGACATTTAAG-3′ (R1914); (*b*) F142 and 5′-GCCTCGCTGGTTCGGTTTTCATG-3′ (R884); (*c*) 5′-AGAAATCAATCAGTAGAAGGCG-3′ (F359) and R884. For RT/PCR of β-actin mRNA, the following primer pair was used: 5′-AACCGCGAGAAGATGACCCAGATCATGTTT-3′ and 5′-AGCAGCCGTGGCCATCTCTTGCTCGAAGTC-3′. For RT/PCR of *Pex* transcripts in bone of normal and *Hyp* mouse, the following primer pairs were used: (*a*) 5′ pair: F142 and R884; (*b*) 3′ pair: 5′-ATCCGACGACTGTCAATGCC-3′ (F1598) and R1914.

To characterize the *Pex* transcript in bone of *Hyp* mice, 10 μg of total RNA isolated from long bone was reverse transcribed as above using an antisense mouse *Pex* primer: 5′-TCTAGACAGTATCTGTTCAAAG-3′ (R2425). The first cDNA amplification reaction was performed with primers 5′-TTCTGTGTTCATCCGTTTGT-3′ (F600) and R2425. A second round of PCR was performed using primers 5′-TTGTATGTGTCCCCTGATGA-3′ (F616) and R2425. Only one round of PCR was necessary to obtain an amplified product with reverse-transcribed RNA from normal mouse bone.

Genomic DNA from normal and *Hyp* mice was PCR amplified with forward primer 5′-GTTCACTTCCAGGAGGTTAAG-3′ (F1273) and reverse primer 5′-ACCACTATTCTGGGTGTTTG-3′ (RI-1). The sequence of RI-1 was based on the putative intronic sequence identified in the *Pex* transcript cloned from *Hyp* mouse bone.

PCR was performed in a DNA Thermal Cycler (480; Perkin-Elmer Corp., Norwalk, CT) with either *Taq* polymerase or ELONGASE (Gibco-BRL) in 1.5 mM $MgCl_2$, 0.2 μM of each primer, 20 μM of each dNTP, as recommended by the supplier. Cycling profiles included an initial denaturating step of 3 min at 94°C followed by 35 cycles at 94°C for 45 sec, 60°C for 2 min, 72°C for 1–3 min, and a final extension at 72°C for 7 min. For long range PCR, ELONGASE was used with extension times of 10–20 min. ELONGASE was also used for 5′- and 3′-RACE (see below) and to generate PCR products designated for sequencing. PCR products were fractionated on 1–2% agarose gels, visualized with ethidium bromide and, in some cases, subcloned into a pCR 2.1 plasmid vector (TA Cloning kit; Invitrogen, San Diego, CA) as recommended by the supplier.

Rapid amplification of cDNA ends (5′- and 3′-RACE). For 5′-RACE, mouse poly(A)$^+$ RNA (1 μg) isolated from bone was reverse transcribed using 200 U of SuperScript with *Pex* primer R884 (see above). The single-strand cDNA was purified and the 5′ end extended for 30 min at 37°C with 30 U of terminal deoxynucleotidyl transferase (Gibco-BRL) in the presence of 0.1 mM dATP and 1.5 mM $CoCl_2$. A first round of PCR was performed using a second *Pex* primer (5′-ATCAGGGGACACATACAAACGG-3′; R633) and a hybrid dT_{20} adapter primer with a 5′ extension anchor (5′-ACCCTTCCGAAGCTTGCACT$_{20}$-3′). A nested amplification was performed using a third *Pex* primer (5′-CAGCCAAGGATAAACCCCATAG-3′; R321) and the anchor primer (5′-ACCCTTCCGAAGCTTGCAC-3′). Several PCR products were obtained as visualized on 1% agarose gels. Southern blotting of the gel and hybridization, with ^{32}P-labeled *Pex* primer F142 as a probe, was used to determine the specific band corresponding to the 5′-RACE product. The latter, a 450-bp fragment, was subcloned into pCR 2.1 vector and sequenced.

The 5′ end of human *PEX* cDNA was obtained by reverse transcribing total RNA (10 μg) from human fetal calvaria using random primers and PCR amplification with a forward *PEX* primer based on the 5′ mouse *Pex* cDNA sequence (5′-AGAGTCTTGAATATCAAACG-3′; F-minus110) and R321. The 431-bp fragment was subcloned into pCR 2.1 vector and sequenced.

For 3′-RACE, mouse and human bone poly(A)$^+$ RNA (1 μg) were reverse transcribed using the dT_{20} adapter primer with the 5′ extension anchor described above. PCR was performed with the anchor primer and the following *Pex* primers: first round 5′-CTCGCAAGTATTTAGCACAGTC-3′ (F1526); second round F1598. The 900-bp products were subcloned into pCR 2.1 vector and sequenced.

DNA sequencing. Subcloned fragments were sequenced at the Sheldon Biotechnology Centre (McGill University) using Thermo Sequenase DNA polymerase (Amersham, Oakville, Ontario) and an ABI 373 automated sequencing system. Double-stranded DNA sequencing of PCR products was performed by the dideoxynucleotide chain termination reaction using the dsDNA Cycle Sequencing System (Gibco-BRL) according to the manufacturer's protocol. Three to four clones of each subcloned fragment were sequenced from both strands using *Pex*/*PEX* primers and T7 and M13 reverse primers. Sequence analysis and alignments were performed using the computer program PC Gene version 6.85.

Ribonuclease protection analysis. The ribonuclease protection assay was performed essentially as described by Gilman (23). A 317-bp cDNA fragment corresponding to nucleotides 567 to 884 of the human *PEX* cDNA sequence and a 246-bp cDNA fragment corresponding to nucleotides 1668–1914 of the mouse *Pex* cDNA sequence were subcloned in pBluescript II KS(-) (Stratagene, La Jolla, CA) and used as templates to generate the 5′-*PEX* and 3′-*Pex* riboprobes, respectively. The plasmids were linearized with BamHI and used to synthesize, in vitro, antisense RNA probes with T3 RNA polymerase and [α-^{32}P]UTP (800 Ci/mmol; ICN, Mississauga, Ontario, Canada).

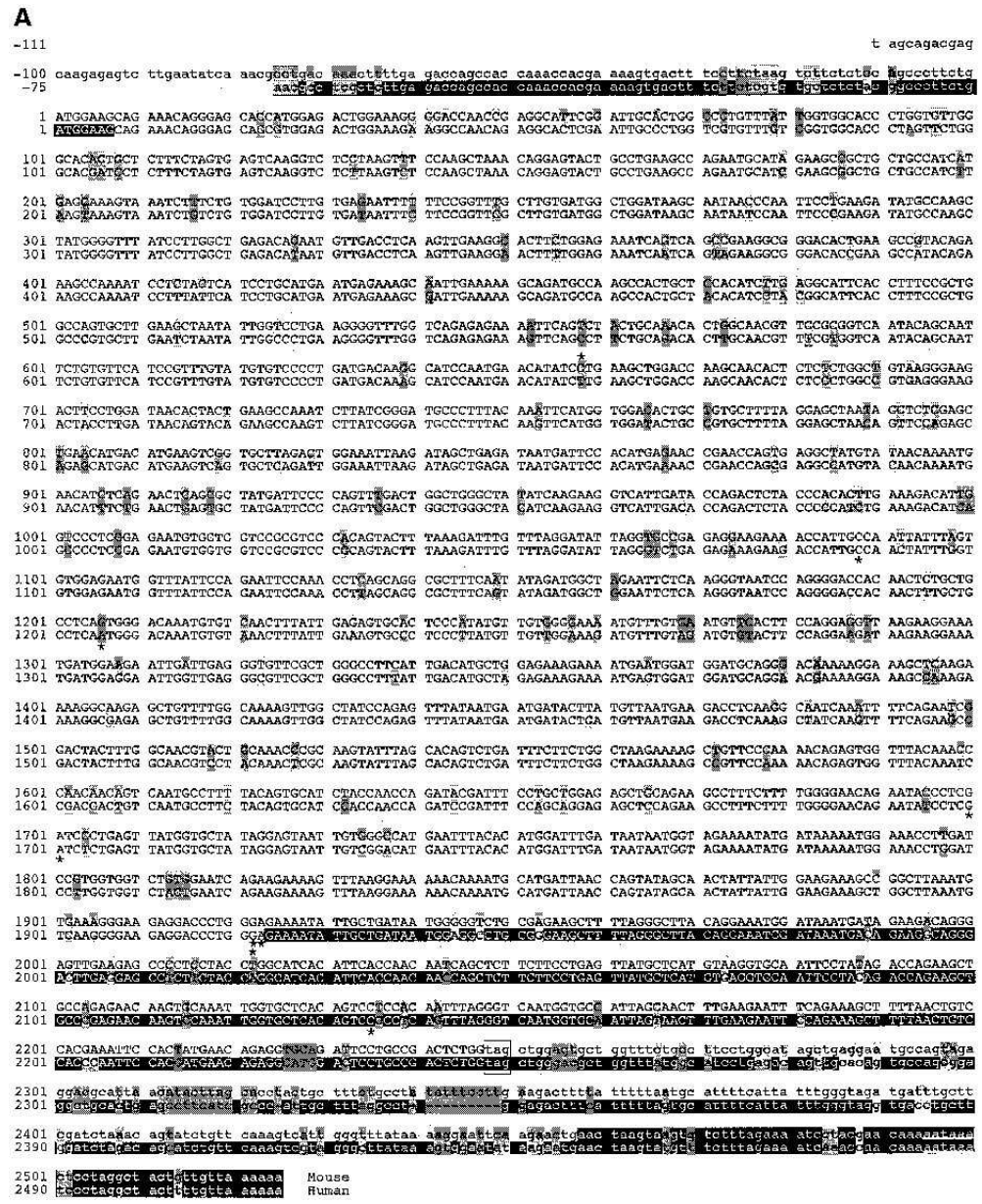

Figure 1. Alignment of nucleotide (*A*) and amino acid (*B*) sequences of mouse and human *Pex*/*PEX* cDNAs and proteins. The polyadenylation sites (*white underline* in *A*), stop codons (*clear box* in *A*), zinc binding motif (*double underline* in *B*), conserved cysteine residues (*clear boxes* in *B*), and nucleotide and amino acid differences between mouse and human (small hatched boxes in *A* and *B*) are shown for each. Nucleotide and amino acid residues not previously published (15, 21) are depicted by boxed-in black areas (*A* and *B*) and differences with published nucleotide and amino acid sequences are indicated by asterisks (*A* and *B*). These data are available from GenBank under accession numbers U75646 and U75645 for the mouse and human *Pex*/*PEX* cDNA sequences, respectively.

The sizes of the 5′-*PEX* and 3′-*Pex* riboprobes were 405 bp and 326 bp, respectively, and that of their RNase T1–protected fragments 320 bp and 245 bp, respectively. As internal standards, a HindIII-KpnI β-actin cDNA fragment, subcloned in pGEM3 (Promega, Madison, WI) and linearized with CvnI, and an XbaI-ApaI GAPDH cDNA fragment subcloned in pBluescript II and linearized with StyI, were used for the synthesis of ^{32}P-labeled antisense riboprobes with T7 RNA polymerase. The sizes of the riboprobes were 160 bp for β-actin and 190 bp for GAPDH and that of the protected fragments 137 bp and 164 bp, respectively. Total RNA (10–20 μg) extracted from various human fetal and mouse tissues was hybridized with the labeled riboprobes (5×10^5 cpm) at 50°C for 18 h and treated with 2 μg/ml RNase T1 at 30°C for 1 h. The protected fragments were precipitated, heat denatured and electrophoresed on a 6% denaturing polyacrylamide gel. The gel was dried and exposed to a PhosphorImager™ screen (Fuji PhosphorImager Bas 2000, Tokyo, Japan) for quantitation and to Kodak Biomax MR1 film for photography. Approximately 30 min exposure was necessary to visualize the β-actin and GAPDH signals whereas a 3–4 d exposure was required for the *Pex/PEX* signal. *Pex*/*PEX* phosphorimage signals were related to those of β-actin or GAPDH under conditions where we previously demonstrated a linear relationship between the quantity of RNA used and the resulting phosphorimage signal.

Northern analysis. Poly(A)$^+$ RNA, prepared from 250 μg of total RNA, was heat denatured and size fractionated on a 1.5% agarose gel containing 18% formaldehyde as previously described (11) and capillary blotted to a Zeta-Probe nylon membrane (BioRad, Mississauga, Ontario). The membrane was ultraviolet irradiated for 2 min and baked under vacuum at 80°C for 30 min. A 1.8-kb mouse *Pex* cDNA fragment, corresponding to nucleotides 142–1914, was labeled by random priming with [α-^{32}P]dCTP and used as probe. Prehybridization (5 min at 49°C) and hybridization (24 h at 49°C) were performed in 50% formamide, 0.12 M Na_2HPO_4, pH 7.2, 0.25 M NaCl, and 7% SDS. Blots were washed to high stringency (final wash in 0.1 × SSC/0.1% SDS, 60°C, 15 min) and exposed to Kodak Biomax MR1 film at −80°C. After stripping, the membranes were rehybridized with a ^{32}P-labeled 1.3-kb β-actin cDNA probe, as described above.

Southern blotting. Mouse genomic DNA was prepared from liver of normal and *Hyp* male mice, as previously described (24). 10 μg of the genomic DNA was digested separately with EcoRI, BamHI, HindIII, PstI, SstI, or a combination thereof, fractionated on 0.7% agarose gels and capillary transferred to nylon-supported nitrocellulose membranes (Optitran BA-(S)85; Schleicher & Schuell, Keene, NH). The membranes were baked under vacuum at 80°C for 2 h. *Pex* cDNA probes (corresponding to nucleotides 142–884 [a], 142–1122 [b], 142–1914 [c], 1163–1668 [d], 1163–1914 [e], 1668–1914 [f], 1668–2425 [g], and 1956–2425 [h] of the *Pex* cDNA) were labeled using [α-^{32}P]dCTP and a DNA labeling kit (RadPrime; Gibco-BRL). Membranes were hybridized (18 h at 42°C) in 40% formamide, 4 × SSC, 5 × Denhardt's, 100 μg/ml denatured herring sperm DNA, 10% dextran sulfate, 1% SDS, and 20 mM Tris, pH 7.6. The membranes were washed to high stringency (final wash in 0.1 × SSC/ 0.1% SDS at 65°C) and exposed to a Kodak Biomax MR1 film at −80°C for 48 h.

Results

Cloning of murine and human Pex/PEX cDNAs. We cloned and sequenced 2.7-kb mouse and human *Pex/PEX* cDNA fragments (Fig. 1 *A*). The 5′ untranslated region (UTR), protein coding region, and 3′ UTR of the mouse and human cDNAs exhibit 77, 91, and 73% identity, respectively. Polyadenylation signals (AATAAA) were identified at nucleotide 2495 of the mouse *Pex* cDNA and nucleotide 2484 of the human *PEX* cDNA. The complete amino acid sequence of the human *PEX* protein is depicted in Fig. 1 *B* and includes NH_2-terminal amino acid residues 1–3 and COOH-terminal amino acid residues 642–749 that were not reported previously (15). Within the additional 108 COOH-terminal amino acids are three cysteine residues that are conserved in NEP (19) and ECE-1 (20). Alignment of the translated murine and human *Pex/PEX* cDNAs demonstrates 96% identity at the amino acid level (Fig. 1 *B*). Both contain a zinc binding motif in the putative extracellular domain (Fig. 1 *B*). Four amino acid differences with the published human sequence (15) were noted (Fig. 1 *B*: Ala 363, Trp 403, Arg 567, and Gly 641) and each of these residues was conserved in the mouse *Pex* protein (Fig. 1 *B*) (21).

Table I. PEX mRNA Expression in Human Fetal Tissues as a Function of Fetal Age

	Age (weeks)									
Tissue	11	12	13	14	15	16	17	18	19	22
Calvaria		+	+[2]	+	+	+[2]	+	+	+	
Bone		+	+			+				
Lung	−	−		+[3]	+[4]	+[4]	+	+	+	
Muscle				+			+	+	+	
Kidney	−	−		−		−[2]	−	−	−	
Liver				−		−			−	
Adrenal			−	−		−			−	
Heart		−		−					−	
Colon						−			−	
Duodenum						−			−	
Testis				−		−				
Ovary									+	
Brain			−		−					
Pancreas						−				
Spleen					−					−
Thymus						−				
Placenta		−		−					−	

Tissues from fetuses ranging from 11 to 22 wk fetal age were used to prepare total RNA. The RNA was reverse transcribed and PCR amplified using *PEX* primers F359 and R884 as described in Methods. An aliquot of each PCR reaction was electrophoresed on 1.5% agarose gels and visualized with ethidium bromide. PCR reactions were scored for the presence (+) or abscence (−) of an amplified *PEX* product. In some age groups, more than one fetus was examined, as indicated by superscript numbers; the latter depict the number of samples in each group.

Pex/PEX mRNA expression in human fetal and murine tissues. We screened a panel of human fetal tissues for *PEX* mRNA expression by RT/PCR. An amplified *PEX* fragment, corresponding to nucleotides 359–884 of the human *PEX* cDNA, was obtained by RT/PCR of RNA from calvaria, long bone, lung, ovary, and muscle (Table I). Although RT/PCR is not strictly quantitative, the data suggest that *PEX* mRNA is more abundant in calvaria and lung than in ovary and muscle (Fig. 2 *A*). We could not detect an RT/PCR product with RNA from kidney, liver, adrenal, heart, colon, testis, brain, duodenum, pancreas, spleen, thymus, and placenta (Table I and Fig. 2 *A*). In contrast, a β-actin RT/PCR product was generated from all tissues examined (Fig. 2 *A* and data not shown). Water blanks and reactions performed in the absence of reverse transcriptase were all negative (Fig. 2 *A* and data not shown). The identity of the *PEX* PCR products from calvaria, lung, ovary, and muscle was confirmed by digestion with PstI; in each case, the expected 212-bp and 314-bp fragments were obtained (Fig. 2 *B*). In addition, we determined that the sequences of the 526-bp amplified fragments from lung and cal-

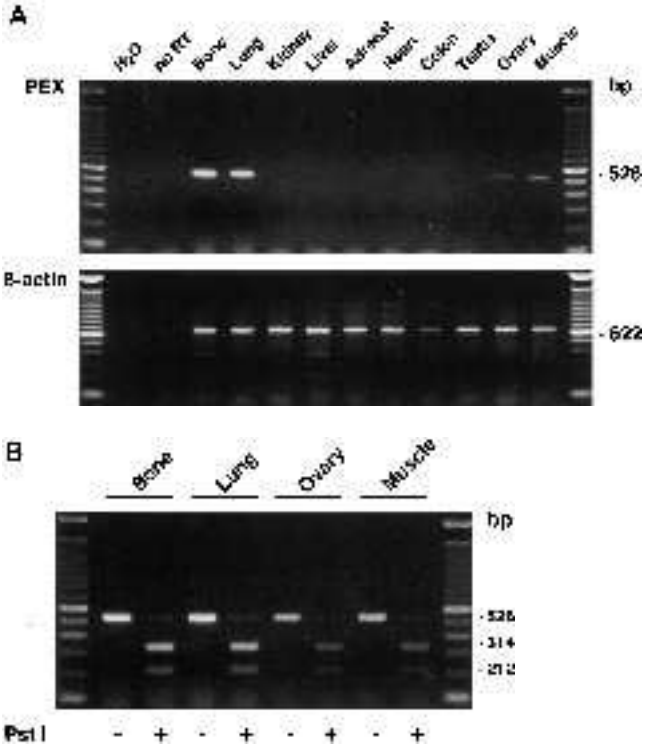

Figure 2. RT/PCR of human fetal tissue RNA. (*A*) Total RNA from human fetal bone (calvaria), lung, kidney, liver, adrenal, heart, colon, testis, ovary, and muscle was reverse transcribed and PCR amplified using *PEX* (F359 and R884, *top*) and β-actin primers (*bottom*) as described in Methods. An aliquot of each PCR reaction was electrophoresed on 1.5% agarose gels and visualized with ethidium bromide. A water blank and an incubation performed in the absence of reverse transcriptase are shown. (*B*) *PEX* RT/PCR products derived from fetal bone (calvaria), lung, ovary, and muscle RNA were incubated in the absence (−) and presence (+) of PstI, electrophoresed, and visualized as described in *A*.

varia were identical to the published *PEX* cDNA sequence (15).

PEX expression data in human fetal tissues, as a function of fetal age, are summarized in Table I. All fetal calvarial (12–19 wk) and long bone (12–16 wk) samples tested were positive for *PEX* mRNA expression. While lung samples from fetuses of 11 and 12 wk fetal age were devoid of detectable *PEX* transcripts, *PEX* mRNA was expressed in all lung samples from 14–19-wk fetuses. RNA samples from skeletal muscle of 14- to 19-wk fetuses were also positive for *PEX* mRNA. In addition, we detected a *PEX* PCR product with reverse-transcribed RNA from an ovary of a 19-wk fetus but found no evidence for *PEX* mRNA expression in testes from 14- and 16-wk fetuses. Significantly, all renal samples examined were devoid of *PEX* mRNA.

PEX mRNA expression in human fetal tissues was also examined by ribonuclease protection assay (Fig. 3). As expected from RT/PCR data, a protected *PEX* fragment of the expected size was observed in calvaria, ovary, lung, and muscle but not in kidney and liver, whereas β-actin protected fragments were detected in all tissues (Fig. 3). By normalizing the protected *PEX* mRNA signal to that of β-actin, we found that the relative abundance of *PEX* mRNA expression in calvaria was approximately sevenfold greater than that in lung, ovary, and muscle ($n = 3$). Similar data were obtained when GAPDH abundance was used to normalize the data ($n = 3$). These results, however, do not take into account tissue-specific differences in β-actin and GAPDH mRNA expression. The exposure time necessary to generate the *PEX* signal was ~ 150 times longer than that for the β-actin and GAPDH signals. These findings suggest that the level of *PEX* mRNA expression in human fetal tissues is at least two orders of magnitude lower than that of β-actin or GAPDH.

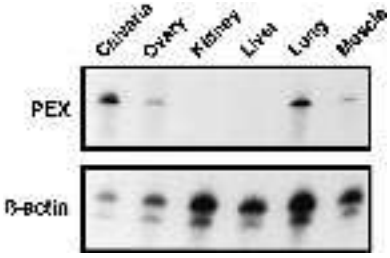

Figure 3. Ribonuclease protection assay of human fetal tissue RNA. Total RNA (10 μg) from human fetal calvaria, ovary, kidney, liver, lung, and muscle was hybridized with ^{32}P-labeled 5′ PEX (Fig. 5 *A*) and β-actin riboprobes and treated with RNase T1 as described in Methods. The protected *PEX* (320-bp) and β-actin (137-bp) fragments were precipitated, electrophoresed on polyacryamide gels, and visualized by autoradiography as described in Methods. A protected *PEX* fragment was never detected in RNA from kidney and liver.

We detected *Pex* transcripts in whole mouse embryo, adult mouse calvaria, long bone and lung, and, to a lesser extent, in adult mouse brain, testis, and muscle by RT/PCR of total RNA (Fig. 4). *Pex* transcripts were not detected in kidney, liver, or heart (Fig. 4). *Pex* mRNA expression in adult mouse bone and lung was also confirmed by ribonuclease protection assay (see Fig. 7, *A* and *B*).

Effect of the Hyp mutation on Pex mRNA expression. Primer pairs from the 5′ (F142 and R884) and 3′ (F1598 and R1914) regions of the mouse *Pex* cDNA (Fig. 5 *A*) were used to amplify reverse transcribed RNA derived from bone of adult normal and *Hyp* mice. With RNA from normal mouse bone, RT/PCR products of the anticipated size were generated with both 5′ and 3′ primer pairs (Fig. 6). In contrast, with RNA isolated from *Hyp* bone, an RT/PCR product of the expected size was obtained with the 5′ but not the 3′ primer pair (Fig. 6). These data suggest that there may be a deletion in the 3′ region of the *Pex* transcript in *Hyp* mice. We used a ribonuclease

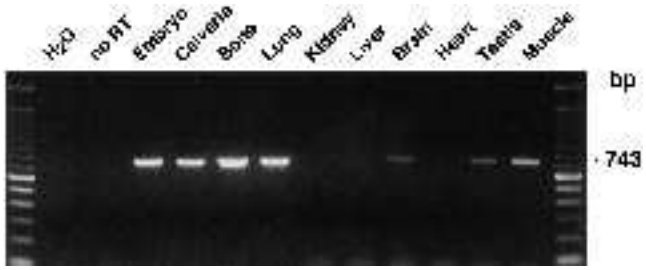

Figure 4. RT/PCR of mouse tissue RNA. Total RNA from whole mouse embryo, adult mouse calvaria, bone, lung, kidney, liver, brain, heart, testis, and muscle, was reverse transcribed and PCR amplified using *Pex*/*PEX* primers (F142 and R884). An aliquot of each PCR reaction was electrophoresed and visualized as described in the legend for Fig. 2.

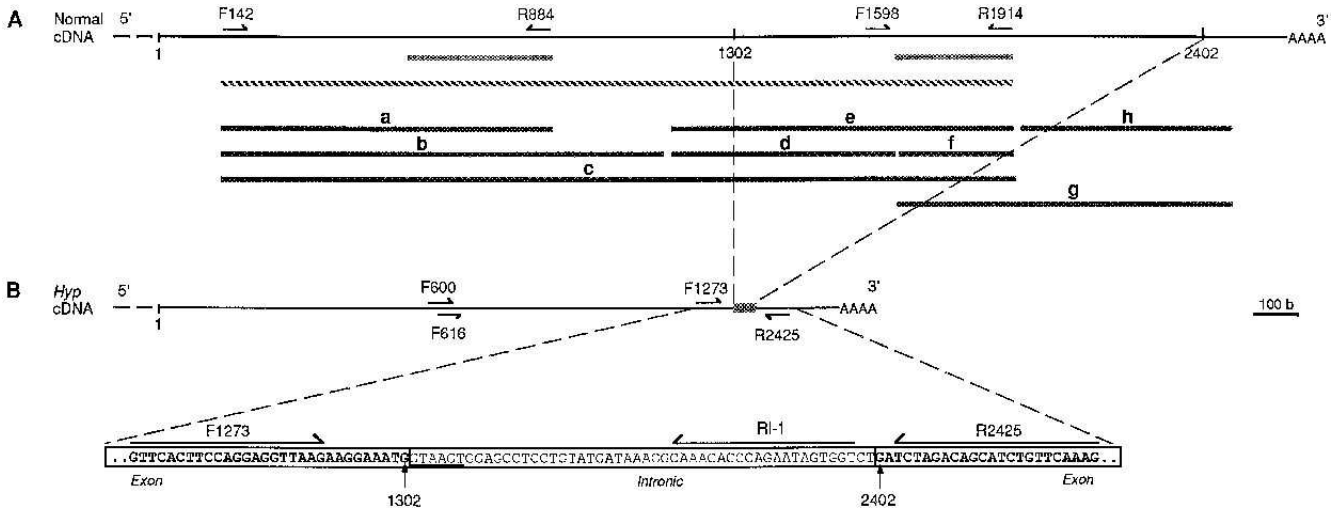

Figure 5. Schematic representation of *Pex* cDNAs from normal (*A*) and *Hyp* (*B*) mice, oligonucleotide primers and probes. (*A*) The 5′ and 3′ primer pairs used to amplify reverse transcribed RNA from normal and *Hyp* mouse bone are shown above the normal *Pex* cDNA. Below the *Pex* cDNA are, first, the 5′ and 3′ riboprobes used in the ribonuclease protection assay; second, the 1.8-kb *Pex* cDNA probe used for Northern analysis; and third, the *Pex* cDNA probes (*a–h*; see Methods) used for Southern analysis. (*B*) A portion of the RT/PCR product derived from RNA of *Hyp* mouse bone and the primers used to generate it are shown. The cDNA sequence that corresponds to *Pex* exon sequence is depicted in bold and the 5′ donor splice site sequence is underlined. Also depicted are the primers (F1273 and RI-1) used to amplify genomic DNA from normal and *Hyp* mice.

protection assay to test this hypothesis. With a *5′-PEX* riboprobe (Fig. 5 *A*), protected *Pex* fragments were detected with RNA isolated from lung and bone, but not liver, of both normal and *Hyp* mice (Fig. 7 *A*). However, with a *3′-Pex* riboprobe (Fig. 5 *A*), a protected *Pex* fragment was detected with RNA from bone and lung of normal mice but not with RNA from the corresponding tissues of *Hyp* mice (Fig. 7 *B*). Protected β-actin fragments were detected in RNA samples isolated from all tissues examined (Fig. 7, *A* and *B*). These results are consistent with the notion that there is a deletion in the 3′ region of the *Pex* transcript in mice harboring the *Hyp* mutation. The ribonuclease protection assay also confirms that *Pex* mRNA is expressed in bone and lung, but not in liver and muscle, of normal adult mice (Fig. 7, *A* and *B*).

To define the boundaries of the putative deletion in the *Pex* transcript of *Hyp* mice, RNA isolated from bone of normal and mutant mice was reverse transcribed with R2425 and

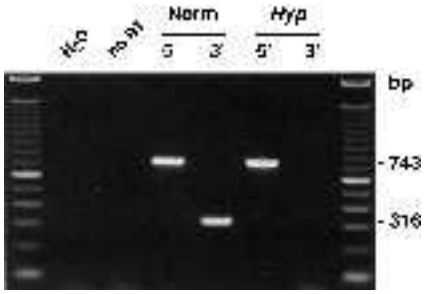

Figure 6. RT/PCR of RNA from bone of normal and *Hyp* mice. Total RNA from long bone of normal and *Hyp* mice was reverse transcribed and PCR amplified with 5′ (F142 and R884) and 3′ (F1598 and R1914) *Pex*/*PEX* primer pairs. An aliquot of each PCR reaction was electrophoresed and visualized as described in the legend for Fig. 2. An RT/PCR product was never detected with RNA from *Hyp* bone using the 3′ primer pair.

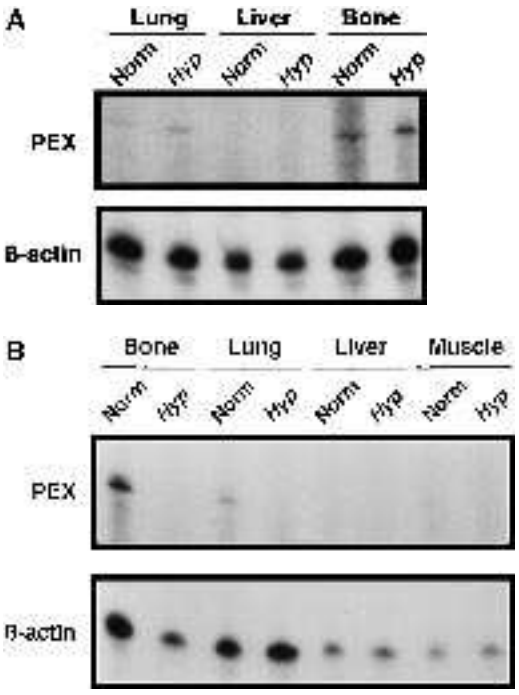

Figure 7. Ribonuclease protection assay of RNA from tissues of normal and *Hyp* mice. (*A*) Total RNA (10 μg) from lung, liver, and bone of normal and *Hyp* mice was hybridized with ^{32}P-labeled 5′ *PEX* and β-actin riboprobes and treated with RNase T1 as described in Methods. Using the 5′ *PEX* riboprobe, protected *Pex* fragments (320-bp) were detected in RNA from both normal and *Hyp* bone and lung. (*B*) Total RNA (20 μg) from bone, lung, liver, and muscle of normal and *Hyp* mice was hybridized with ^{32}P-labeled 3′ *Pex* and β-actin riboprobes and treated as described in (*A*). Using the 3′ *Pex* riboprobe, protected *Pex* fragments (245-bp) were only detected in RNA from normal bone and lung. There was no evidence for a protected *Pex* fragment in RNA from either liver or muscle of normal and *Hyp* mice. Protected β-actin fragments (137-bp) were detected in RNA from all tissues examined (*A* and *B*).

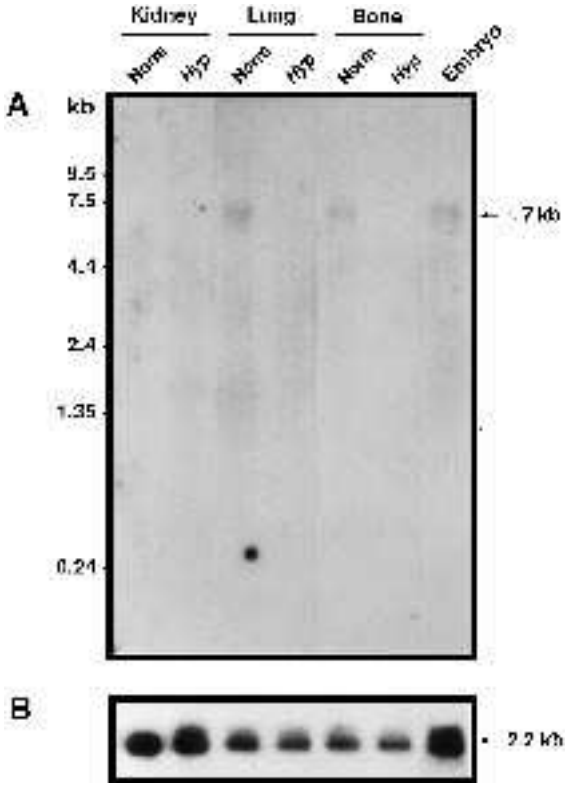

Figure 8. Northern blot analysis of poly(A)$^+$ RNA from kidney, lung, and bone of normal and *Hyp* mice and from normal mouse embryo. After electrophoresis on agarose/formaldehyde gels, poly(A)$^+$ RNA was transferred to a nylon membrane and hybridized sequentially with ^{32}P-labeled 1.8-kb *Pex* and 1.3-kb β-actin cDNA probes as described in Methods. *Pex* and β-actin mRNAs were visualized by autoradiography. Size of *Pex* and β-actin transcripts is shown. Exposure times to visualize *Pex* and β-actin transcripts were 4 d and 2 h, respectively.

PCR amplified with F616 and R2425 (Fig. 5 *B*). The amplified product from *Hyp* bone was ≈ 1 kb shorter than that from normal bone. The sequence of the RT/PCR product from *Hyp* bone was identical to that of normal *Pex* cDNA between nucleotides 616 and 1302 (Fig. 5 *B*). However, the next 48 bases in the amplified product from *Hyp* bone were not found in mouse *Pex* cDNA (Fig. 5 *B*). The first six bases in this region, GTAAGT, were typical of a splice donor site sequence, suggesting that nucleotide 1302 is at the junction of an exon/intron boundary in the *Pex* gene and that the 48 bases comprise part of an intron that is retained in the mutant *Pex* transcript (Fig. 5 *B*). Indeed, using primer F1273 and a reverse primer from within the putative intron (RI-1, Fig. 5 *B*), we were able to amplify, from genomic DNA of both normal and *Hyp* mice, a PCR product with a sequence identical to that present in the aberrant *Hyp* transcript (Fig. 5 *B*). In addition, using primers F616 and RI-1, we were able to RT/PCR a cDNA fragment of the expected size with RNA from *Hyp*, but not normal, bone (data not shown). Immediately following the 48 bases of the intron are two bases, GA, followed by the reverse primer, R2425, sequence (Fig. 5 *B*). Taken together, the data suggest that the *Pex* transcript in *Hyp* mice is characterized by an interruption in the normal *Pex* cDNA sequence at nucleotide 1302 and the retention of at least 48 bases from the adjacent intron.

Northern analysis of poly (A)$^+$ RNA was performed to compare the sizes of the *Pex* transcripts in normal and *Hyp* mouse bone and lung. A very low-abundance *Pex* transcript of ≈ 7 kb was detected in bone and lung of normal adult mice and in normal mouse embryo (Fig. 8). However, we could not detect a *Pex* transcript in bone and lung of *Hyp* mice (Fig. 8). Neither mouse strain expressed *Pex* mRNA in kidney (Fig. 8), in agreement with RT/PCR data (Fig. 4). A 2.2-kb transcript was evident in all lanes upon rehybridization of the Northern blot with a β-actin cDNA probe, confirming the integrity of the mRNA, particularly in those samples devoid of *Pex* transcript (Fig. 8).

Southern analysis of genomic DNA from normal and *Hyp* mice was performed to determine whether the deletion in the *Pex* transcript was the result of a major rearrangement in the *Pex* gene. The *Pex* cDNA probes tested (*a–h*, Fig. 5 *A*) fell into three distinct groups with respect to their hybridization patterns with normal and *Hyp* DNA. With probes a, b, and d, similar hybridization patterns were obtained with normal and *Hyp* DNA (e.g., Fig. 9 *A*). With probes c and e, some but not all bands were absent with DNA from *Hyp* mice (e.g., Fig. 9 *B*). However, with probes f, g, and h from the 3′ region of the *Pex* cDNA, no hybridization signal was detected with DNA from *Hyp* mice (e.g., Fig. 9 *C*). Based on the position of the probes tested and the Southern blots generated, we conclude that there is a 3′ deletion in the *Pex* gene of *Hyp* mice and suggest that the deletion occurs around nucleotide 1668 of the *Pex* cDNA. Based on the sizes of missing bands with probes c, e, f, g, and h, we estimate that the *Pex* deletion in *Hyp* mice is between 18 and 33 kb.

Discussion

The HYP consortium recently identified a candidate gene, *PEX*, for XLH by positional cloning (15). While more than 25 mutations in the *PEX* gene have been identified in patients with XLH (15–18), the genetic basis for the murine *Hyp* homologue of the human disease is not known. Moreover, no information about *PEX* tissue distribution was provided by the consortium and only a partial *PEX* cDNA was isolated (15). In the present study, we cloned murine and human *Pex*/*PEX* cDNAs comprising part of the 5′ UTR, the complete protein coding region and the entire 3′ UTR, we examined the distribution of *Pex*/*PEX* mRNA in human fetal and murine tissues and defined the nature of the *PEX* mutation in mice harboring the X-linked *Hyp* mutation. We show that *Pex* is a very low-abundance transcript of ≈ 7 kb that is preferentially expressed in bone and that the *Hyp* mutation results from a large deletion in the 3′ region of the *Pex* gene.

The preferential expression of *Pex*/*PEX* in bone is of interest and consistent with the presence of bone disease in XLH patients and *Hyp* mice. Previous studies have shown that histomorphometric parameters of bone formation are not normalized after transplantation of bone cells from *Hyp* mice into the gluteal muscle of normal mice or phosphate-supplemented *Hyp* mice (25–27). These data suggest that the hypophosphatemic environment, arising from the renal phosphate leak, is not sufficient for the bone disease in *Hyp* mice. Additional evidence for an intrinsic bone defect in *Hyp* mice was derived from the demonstration that gluconeogenesis is abnormally elevated and steady state intracellular pH is significantly decreased in cultured osteoblasts derived from *Hyp* mice when

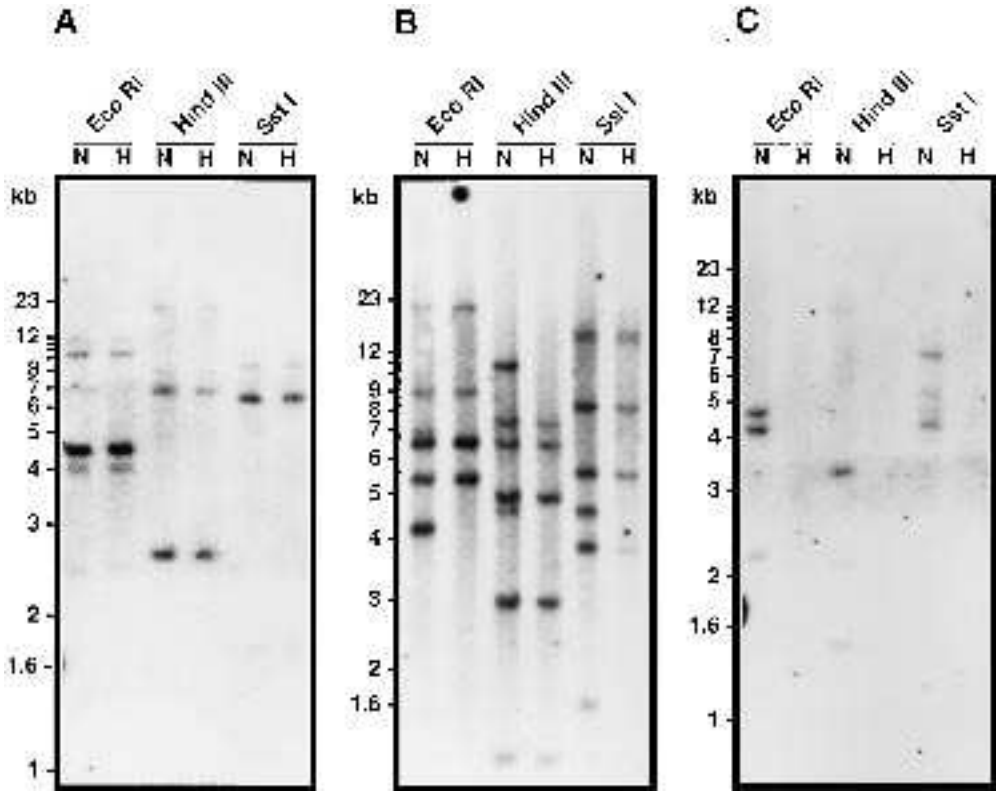

Figure 9. Southern blot analysis of genomic DNA from normal and *Hyp* mice. DNA (10 μg) was digested to completion with EcoRI, HindIII, or SstI, electrophoresed on 0.7% agarose gels, transferred to a supported nitrocellulose membrane, and hybridized with ^{32}P-labeled *Pex* cDNA probes b (*A*), e (*B*), and g (*C*) as described in Methods. The probes are depicted in Fig. 5 *A*. A size calibration was obtained by simultaneous loading of lambda DNA/HindIII fragments and a 1-kb DNA ladder.

compared with normal osteoblasts (28, 29). While further work is necessary to identify the precise function of *Pex*/*PEX* in bone and the mechanism whereby loss of *Pex*/*PEX* function mediates the bone abnormalities in XLH and *Hyp*, our data clearly show that *Pex*/*PEX* is expressed early in bone development.

Studies in the *Hyp* mouse demonstrated that the renal defect in phosphate transport in not intrinsic to the kidney but rather depends on a circulating factor for its expression (30, 31). The present demonstration that *Pex*/*PEX* is not expressed in kidney is consistent with these findings and suggests that *Pex*/*PEX* expression at extrarenal site(s) is involved in the processing/inactivation of an endocrine factor that is involved in the regulation of renal phosphate handling. Additional studies are required to identify the *Pex*/*PEX* substrate and to assess the contribution of *Pex*/*PEX* expression at sites other than bone (e.g., lung) in the regulation of renal phosphate reabsorption. Moreover, the relationship between the *Pex*/*PEX* substrate and phosphotonin, the putative phosphaturic factor produced by tumors from patients with oncogenic hypophosphatemic osteomalacia (tumor-induced osteomalacia), remains to be established (32, 33).

In the present study, we provide evidence for a deletion in the 3′ region of the *Pex* gene in *Hyp* mice using a variety of approaches. RT/PCR (Fig. 6) and ribonuclease protection assays (Fig. 7, *A* and *B*) clearly demonstrate the presence of 5′ but not 3′ sequences in the *Pex* transcript derived from *Hyp* bone. Analysis of the RT/PCR product demonstrates the absence of *Pex* cDNA sequence downstream from nucleotide 1302 of the normal *Pex* cDNA (Fig. 5 *B*). Finally, we show by Southern analysis that genomic DNA from *Hyp* mice does not hybridize with probes from the 3′ region of the *Pex* cDNA (Fig. 9 *C*). Based on the data from Southern analyses, we estimate that the deletion in the 3′ region of the *Pex* gene in *Hyp* mice is between 18 and 33 kb. Our findings are consistent with those described in an abstract by Strom et al. (34) in which a deletion of the 3′ end of the *Pex* gene was reported in *Hyp* mice. However, our findings are at odds with a recent report by Du et al. (21) in which no mutation was detected in the *Pex* cDNA generated by RT/PCR of RNA from *Hyp* mouse bone. While Du et al. suggested that the *Hyp* mutation may reside in either an untranslated region or in the promoter of the *Pex* gene, one cannot rule out the possibility that their results are due to contamination with normal *Pex* cDNA, given the sensitivity of PCR assays (21).

We demonstrate that at least 48 bases of intron sequence are retained in the *Pex* transcript derived from *Hyp* mouse bone and that the intron sequence is found downstream from nucleotide 1302 of the normal *Pex* cDNA. Evidence supporting this conclusion was derived from sequence analysis of PCR products generated from genomic DNA of normal or *Hyp* mice, using primers that flank the exon/intron junction at nucleotide 1302 (F1273 and RI-1, a reverse primer from the putative intron region [Fig. 5 *B*]). However, we could not PCR amplify the intron that is retained in the *Pex* transcript of *Hyp* mice or estimate the size of the deletion in the *Pex* gene by long range PCR of normal and *Hyp* genomic DNA, using primer F1273 in combination with several reverse primers from the 3′ region of the *Pex* cDNA. Because we were able to PCR amplify an 11-kb fragment of the *Npt2* gene (24) using the same genomic DNA templates, we conclude that the intron in question and the deletion are very large and/or that all the reverse primers tested span an intron/exon junction. Both are likely possibilities given that the *Pex* gene is very large and

is comprised of many small exons, as is the case for the homologous gene encoding NEP (35).

The precise mechanism for the retained intron sequence in the *Pex* transcript of *Hyp* mice is unclear. A recent survey of splice mutations found that only 6% are associated with intron retention in the aberrant transcript (36). In most instances, intron retention can be ascribed to mutations in the 5′ donor splice site (36–38), which is clearly not the mechanism operating in *Hyp.* However, there are at least two reports in which intron retention is associated with deletions in intron sequences that result in the activation of cryptic donor and acceptor splice sites (39, 40). This latter mechanism may indeed explain the present findings in the *Hyp* mouse.

The sequence downstream from the 48 bases of the retained intron in the aberrant *Pex* transcript of *Hyp* mice consists of GA followed by the sequence of the reverse primer (R2425) used to generate the PCR product. This may represent the true *Pex* transcription product in *Hyp* mice. Alternatively, the mutant RT/PCR product may be the result of an amplification reaction in which the reverse primer annealed to an unrelated but partially complementary sequence in the retained intron. Since the structure of the *Pex* gene is not known, we cannot distinguish between these possibilities at present. In any case, the aberrant *Pex* transcript in *Hyp* mice is likely to be highly unstable and this may explain why we were unable to detect the aberrant transcript by Northern analysis of poly $(A)^+$ RNA from *Hyp* mouse bone and lung (Fig. 8). The latter findings are consistent with the results of Du et al. who also failed to detect a *Pex* transcript on Northern blots of total RNA isolated from *Hyp* mouse bone (21).

In summary, we have shown that *Pex*/*PEX* is a very low-abundance transcript of $\sim$ 7 kb that is preferentially expressed in bone of mice and humans. We have also presented evidence for a large deletion in the 3′ region of the *Pex* gene in mice harboring the X-linked *Hyp* mutation. Our data are consistent with the absence of functional *Pex* protein in *Hyp* mice and support the hypothesis that loss of *Pex* function is responsible for the mutant *Hyp* phenotype.

Acknowledgments

We thank Dr. B. Escoubet (Institut National de la Santé et de la Recherche Médicale U 251, Paris, France) for her ribonuclease protection assay protocol and gift of β-actin and GAPDH plasmids for the preparation of the corresponding riboprobes. We also thank Drs. P. Crine, G. Boileau, and L. DesGroseillers (Université de Montréal, Montreal, Quebec) for advice and primers for 5′ and 3′ RACE, and Julie Tranchemontagne, a summer student, for setting up the Southern blot technique.

This work was supported by grants from the Medical Research Council of Canada (MRC Group Grant in Medical Genetics) and the Kidney Foundation of Canada. Laurent Beck is the recipient of a Fellowship Award from the McGill University-Montreal Children's Hospital Research Institute.

References

1. McKusick, V.A. 1992. Mendelian Inheritance in Man. Johns Hopkins University Press, Baltimore. 1871–1873.

2. Rasmussen, H., and H. S. Tenenhouse. 1995. Mendelian hypophosphatemias. *In* The Metabolic and Molecular Basis of Inherited Disease. C.R. Scriver, A.L. Beaudet, W.S. Sly, and D. Valle, editors. McGraw Hill Book Co., New York. 3717–3745.

3. Eicher, E.M., J.L. Southard, C.R. Scriver, and F.H. Glorieux. 1976. Hypophosphatemia: mouse model for human familial hypophosphatemic (vitamin D-resistant) rickets. *Proc. Natl. Acad. Sci. USA.* 73:4667–4671.

4. Tenenhouse, H.S., and C.R. Scriver. 1992. X-linked hypophosphatemia. A phenotype in search of a cause. *Int. J. Biochem.* 24:685–691.

5. Tenenhouse, H.S., and J. Martel. 1993. Renal adaptation to phosphate deprivation: lessons from the X-linked *Hyp* mouse. *Ped. Nephrol.* 7:312–318.

6. Scriver, C.R., and H.S. Tenenhouse. 1990. Conserved loci on the X chromosome confer phosphate homeostasis in mice and humans. *Genet. Res. (Camb.).* 56:141–152.

7. Tenenhouse, H.S., A.H. Klugerman, and J.L. Neal. 1989. Effect of phosphonoformic acid, dietary phosphate and the *Hyp* mutation on kinetically distinct phosphate transport processes in mouse kidney. *Biochim. Biophys. Acta.* 984:207–213.

8. Tenenhouse, H.S., A. Werner, J. Biber, S. Ma, J. Martel, S. Roy, and H. Murer. 1994. Renal Na^+-phosphate cotransport in murine X-linked hypophosphatemic rickets: molecular characterization. *J. Clin. Invest.* 93:671–676.

9. Tenenhouse, H.S., A. Yip, and G. Jones. 1988. Increased renal catabolism of 1,25-dihydroxyvitamin D_3 in murine X-linked hypophosphatemic rickets. *J. Clin. Invest.* 81:461–465.

10. Tenenhouse, H.S., and G. Jones. 1990. Abnormal regulation of renal vitamin D catabolism by dietary phosphate in murine X-linked hypophosphatemic rickets. *J. Clin. Invest.* 85:1450–1455.

11. Roy, S., J. Martel, S. Ma, and H.S. Tenenhouse. 1994. Increased renal 25-hydroxyvitamin D_3-24-hydroxylase messenger ribonucleic acid and immunoreactive protein in phosphate-deprived *Hyp* mice: a mechanism for accelerated 1,25-dihydroxyvitamin D_3 catabolism in X-linked hypophosphatemic rickets. *Endocrinology.* 134:1761–1767.

12. Roy, S., and H.S. Tenenhouse. 1996. Transcriptional regulation and renal localization of 1,25-dihydroxyvitamin D_3-24-hydroxylase gene expression: effects of the *Hyp* mutation and 1,25-dihydroxyvitamin D_3. *Endocrinology.* 137: 2938–2946.

13. Kos, C.H., F. Tihy, M.J. Econs, H. Murer, N. Lemieux, and H.S. Tenenhouse. 1994. Localization of a renal sodium phosphate cotransporter gene to human chromosome 5q35. *Genomics.* 19:176–177.

14. Labuda, M., N. Lemieux, F. Tihy, C. Prinster, and F.H. Glorieux. 1993. Human 25-hydroxyvitamin D 24-hydroxylase cytochrome P_{450} subunit maps to a different chromosomal location than that of pseudovitamin D-deficient rickets. *J. Bone Miner. Res.* 8:1397–1406.

15. The HYP Consortium. 1995. A gene (PEX) with homologies to endopeptidases is mutated in patients with X-linked hypophosphatemic rickets. *Nature Genetics.* 11:130–136.

16. Dixon, P.H., C. Wooding, D. Trump, D. Schlessinger, M.P. Whyte, and R.V. Thakker. 1996. Eleven novel mutations in the PEX gene indicate molecular heterogeneity for X-linked hypophosphataemic rickets. *Am. J. Hum. Genet.* 59:256*a.* (Abstr.)

17. Mokrzycki, A.K., M. Tassabehji, M. Davies, P. Rowe, E.B. Mawer, and A.P. Read. 1996. PEX mutations in families with X-linked hypophosphatemic rickets. *Am. J. Hum. Genet.* 59:273*a.* (Abstr.)

18. Holm, L.A., X. Huang, N.M. Zacconi, and L.M. Kunkel. 1996. Mutations in the PEX gene in X-linked hypophosphatemic rickets. *Am. J. Hum. Genet.* 59:43*a.* (Abstr.)

19. Roques, B.P., F. Noble, V. Daugé, M. Fournié-Zaluski, and A. Beaumont. 1993. Neutral endopeptidase 24.11: structure, inhibition, and experimental and clinical pharmacology. *Pharmacol. Rev.* 45:87–146.

20. Xu, D., N. Emoto, A. Giaid, C. Slaughter, S. Kaw, D. deWit, and M. Yanagisawa. 1994. ECE-1: A membrane-bound metalloprotease that catalyzes the proteolytic activation of big endothelin-1. *Cell.* 78:473–485.

21. Du, L., M. Desbarats, J. Viel, F.H. Glorieux, C. Cawthorn, and B. Ecarot. 1996. cDNA cloning of the murine *Pex* gene implicated in X-linked hypophosphatemia and evidence for expression in bone. *Genomics.* 36:22–28.

22. Munsick, R.A. 1984. Human fetal extremity lengths in the interval from 9 to 21 menstrual weeks of pregnancy. *Am. J. Obstet. Gynecol.* 149:883–887.

23. Gilman, M. 1993. Ribonuclease protection assay. *In* Current Protocols in Molecular Biology. A.U. Ausubel, R. Brent, R.E. Kingston, D.D. Moore, J.G. Seidman, J.A. Smith, and K. Struhl, editors. John Wiley and Sons, New York. Vol 1, unit 4.7, 1–8.

24. Hartmann, C.M., A.S. Hewson, C.H. Kos, H. Hilfiker, Y. Soumoumou, H. Murer, and H.S. Tenenhouse. 1996. Structure of murine and human renal type II Na^+-phosphate cotransporter genes (*Npt2* and NPT2). *Proc. Natl. Acad. Sci. USA.* 93:7409–7414.

25. Ecarot-Charrier, B., F.H. Glorieux, R. Travers, M. Desbarats, F. Bouchard, and A. Hinek. 1988. Defective bone formation by transplanted *Hyp* mouse bone cells into normal mice. *Endocrinology.* 123:768–773.

26. Ecarot, B., F.H. Glorieux, M. Desbarats, R. Travers, and L. Labelle. 1992. Defective bone formation by *Hyp* mouse bone cells transplanted into normal mice: evidence in favor of an intrinsic osteoblast defect. *J. Bone Miner. Res.* 7:215–220.

27. Ecarot, B., F.H. Glorieux, M. Desbarats, R. Travers, and L. Labelle. 1992. Effect of dietary phosphate deprivation and supplementation of recipient mice on bone formation by transplanted cells from normal and X-linked hypophosphatemic mice. *J. Bone Miner. Res.* 7:523–530.

28. Hruska, K.A., L. Rifas, S.-L. Cheng, A. Gupta, L. Halstead, and L. Avi-

oli. 1995. X-linked hypophosphatemic rickets and the murine *Hyp* homologue. *Am. J. Physiol.* 268:F357–F362.

29. Rifas, L., A. Gupta, K.A. Hruska, and L.V. Avioli. 1995. Altered osteoblast gluconeogenesis in X-linked hypophosphatemic mice is associated with a depressed intracellular pH . *Calcif. Tissue Int.* 57:60–63.

30. Meyer, R.A., Jr., H.S. Tenenhouse, M.H. Meyer, and A.H. Klugerman. 1989. The renal phosphate transport defect in normal mice parabiosed to X-linked hypophosphatemic mice persists after parathyroidectomy. *J. Bone Miner. Res.* 4:523–532.

31. Nesbitt, T., T.M. Coffman, R. Griffiths, and M.K. Drezner. 1992. Cross-transplantation of kidneys in normal and *Hyp* mice: evidence that the *Hyp* phenotype is unrelated to an intrinsic renal defect. *J. Clin. Invest.* 89:1453–1459.

32. Cai, Q., S.F. Hodgson, P.C. Kao, V.A. Lennon, G.G. Klee, A.R. Zinsmiester, and R. Kumar. 1994. Brief report: inhibition of renal phosphate transport by a tumor product in a patient with oncogenic osteomalacia. *N. Engl. J. Med.* 330:1645–1649.

33. Econs, M.J., and M.K. Drezner. 1994. Tumor-induced osteomalacia: unveiling a new hormone. *N. Engl. J. Med.* 330:1679–1681.

34. Strom, T.M., F. Francis, B. Lorenz, A. Boeddrich, M. Econs, T. Guenther, H. Lehrach, and T. Meitinger. 1996. Hyp and Gy, the mouse models for hypophosphatemic rickets, are allelic mutations. *Am. J. Hum. Genet.* 59:286*a.* (Abstr.)

35. D'Adamio, L., M.A. Shipp, E.L. Masteller, and E.L. Reinherz. 1989. Organization of the gene encoding common acute lymphoblastic leukemia antigen (neutral endopeptidase 24.11): multiple miniexons and separate 5′ untranslated regions. *Proc. Natl. Acad. Sci. USA.* 86:7103–7107.

36. Nakai, K., and H. Samamoto. 1994. Construction of a novel database containing aberrant splicing mutations of mammalian genes. *Gene.* 141:171–177.

37. Stover, M.L., D. Primorac, S.C. Liu, M.B. McKinstry, and D.W. Rowe. 1993. Defective splicing of mRNA from one COL1A1 allele of type 1 collagen in nondeforming (type 1) osteogenesis imperfecta. *J. Clin. Invest.* 92:1994–2002.

38. Morrone, A., H. Morreau, X.Y. Zhou, E. Zammarchi, W.J. Kleijer, H. Galjaard, and A. d'Asso. 1994. Insertion of a T next to the donor splice site of intron 1 causes aberrantly spliced mRNA in a case of infantile GM_1-gangliosidos. *Hum. Mut.* 3:112–120.

39. Peral, B., V. Gamble, J.L. San Millan, C. Strong, J. Sloane-Stanley, F. Moreno, and P.C. Harris. 1995. Splicing mutations of the polycystic kidney disease 1 (*PKD1*) gene induced by intronic deletion. *Hum. Molec. Genet.* 4:569–574.

40. Hou, S. 1994. Novel types of mutation identified at the hprt locus of human T-lymphocytes. *Mut. Res.* 308:23–31.